Interaction of a Magainin−PGLa Hybrid Peptide with Membranes: Insight into the Mechanism of Synergism†

Minoru Nishida,‡ Yuichi Imura,§ Megumi Yamamoto,§ Satoe Kobayashi,§,|| Yoshiaki Yano,§ and Katsumi Matsuzaki*,§

Graduate School of Pharmaceutical Sciences and Graduate School of Biostudies, Kyoto University, Sakyo-ku, Kyoto 606-8501, Japan

Received September 11, 2007; Revised Manuscript Received October 4, 2007

ABSTRACT: The antimicrobial peptides magainin 2 and PGLa isolated from the skin of the African clawed frog *Xenopus laevis* show marked functional synergism. We have proposed that the two peptides form a heterodimer composed of parallel helices with strong membrane permeabilizing activity [Hara, T., Mitani, Y., Tanaka, K., Uematsu, N., Takakura, A., Tachi, T., Kodama, H., Kondo, M., Mori, H., Otaka, A., Fujii, N., and Matsuzaki, K. (2001) *Biochemistry 40*, 12395−12399]. In this study, to elucidate the molecular mechanism of the synergy, we synthesized a chemically fixed heterodimer and investigated in detail the interaction of the hybrid peptide with bacteria, erythrocytes, and lipid bilayers. The hybrid peptide showed antimicrobial activity and membrane permeabilizing activity against negatively charged membranes, similar to or even stronger than those of a physical equimolar mixture of magainin and PGLa, indicating that the synergy is due to the formation of a parallel heterodimer. The heterodimer assumed a more oblique orientation than the component peptides. In contrast, the cross-linking of the two peptides significantly strengthened the action against erythrocytes and zwitterionic lipid bilayers by enhancing the affinity for membranes without changing the basic mode of action. Thus, the separate production of mutually recognizing peptides without cross-linking appears to be a good way to increase selective toxicity.

Several hundred antimicrobial peptides have been discovered in both the animal and plant kingdoms and are expected to be promising candidates for novel antibiotics, because they exhibit broad antimicrobial spectra and high selective toxicity (*1*−*3*). Most of these peptides potentially form polycationic amphipathic structures, such as α-helices and *β*-sheets, that can bind to and permeabilize negatively charged bacterial membranes. One of the most studied peptide groups is the magainin peptide family (*4*), including magainin 2 (*5*) and PGLa (*6*) isolated from the skin of the African clawed frog *Xenopus laevis* (Figure 1). Our group has proposed the following mechanisms for membrane permeabilization induced by these peptides (*4*, *7*, *8*). The peptide forms an amphipathic helix in lipid bilayers, which essentially lies parallel to the membrane surface (*9*), imposing positive curvature strain on the membrane (*10*). To release this stress, several helices together with several surrounding lipids form a membrane-spanning pore comprising a dynamic, peptide−lipid supramolecular complex (toroidal pore), which allows not only ion transport but also rapid flip-flop of the membrane lipids (*11*). The structure of the pore has been determined by neutron diffraction (*12*). Upon disintegration of the pore, a fraction of the peptide molecules stochastically translocate into the inner leaflet (*13*, *14*). Antiparallel homodimers of magainin peptides have been suggested to play an important role in pore formation (*15*, *16*).

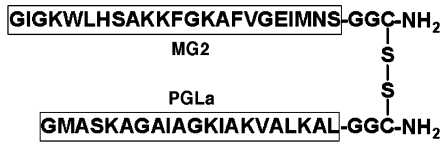

FIGURE 1: Structure of the MG2−PGLa hybrid peptide. The sequences surrounded with frames indicate MG2 and PGLa moieties.

There are several reports that the combined use of two antimicrobial peptides results in synergism, although the underlying mechanisms are yet to be elucidated (*17*−*21*). The best known example is the equimolar mixture of magainin 2 and PGLa, which shows marked functional synergism in bacteria, tumor cells, and artificial lipid membranes (*22*−*26*) and becomes hemolytic, losing the selectivity of magainin 2 and PGLa alone (*18*). We suggested previously that these peptides form a 1/1 stoichiometric complex in membranes with a Gibbs free energy of −15 kJ/mol (*26*) based on spectroscopic measurements. Indeed, our cross-linking experiments showed that magainin 2 and PGLa form a heterodimer composed of parallel helices with strong membrane permeabilizing activity, although there is no information about the orientation between adjacent heterodimers in the pore (*27*).

† Supported in part by the Inamori Foundation, the Shimizu Foundation for the Promotion of Immunology Research, and a Grant-in-Aid for Scientific Research (14572091) from the Ministry of Education, Culture, Sports, Science and Technology of Japan.

* To whom correspondence should be addressed. Telephone: 81-75-753-4521. Fax: 81-75-753-4578. E-mail: katsumim@pharm.kyoto-u.ac.jp.

‡ Graduate School of Biostudies.

§ Graduate School of Pharmaceutical Sciences.

|| Current address: Faculty of Pharmaceutical Sciences, Toyama University, 930-0194 Toyama, Japan.

10.1021/bi701850m CCC: $37.00
Published on Web 11/16/2007

In this study, to elucidate the molecular mechanism of the synergy, we synthesized a chemically fixed heterodimer (Figure 1) and investigated in detail the interaction of the hybrid peptide with bacteria, erythrocytes, and lipid bilayers. The use of the fixed dimer is essential, because only a fraction of the peptides forms the heterodimer in a physical 1/1 mixture of magainin 2 and PGLa (*26*). The hybrid peptide exhibited antimicrobial activity and membrane permeabilizing activity against negatively charged membranes, similar to or even stronger than those of a physical equimolar mixture of magainin and PGLa, indicating that the synergy is due to the formation of a parallel heterodimer. In contrast, the cross-linking of the two peptides significantly strengthened the action against erythrocytes and zwitterionic lipid bilayers by enhancing the affinity for membranes without changing the basic mode of action. The heterodimer assumed a more oblique orientation than the component peptides, especially in zwitterionic membranes.

MATERIALS AND METHODS

Peptides. The peptides were custom synthesized and characterized by Peptide Institute (Minou, Japan). The purity of the peptides was greater than 95%. A Trp residue was introduced into magainin 2 and PGLa to fluorometrically monitor peptide−membrane interactions. F5W-Magainin 2 (MG2)[1] (*9*) and L18W-PGLa (*26*) have been confirmed to be equipotent to the parent peptides. The parallel heterodimer, which is spontaneously formed by mixing MG2-Gly-Gly-Cys-amide and PGLa-Gly-Gly-Cys-amide in phospholipid membranes (*27*), was formed by selectively cross-linking the Cys residues (Figure 1). The corresponding component monomer peptides with the Gly-Gly-Cys linker exhibited membrane permeabilizing activities similar to those of MG2 and PGLa (*27*). Thus, the heterodimer is expected to be a good model for the putative magainin 2−PGLa complex. The peptide concentration of the dimer was expressed as the concentration reduced to monomer throughout this study. Namely, 1 mol of hybrid peptide is counted as 2 mol of monomer peptide.

Other Materials. Egg yolk L-α-phosphatidylcholine (EYPC), L-α-phosphatidyl-DL-glycerol enzymatically converted from EYPC (EYPG), carbonyl cyanide *m*-chlorophenylhydrazone (CCCP), and polymixin B sulfate were obtained from Sigma (St. Louis, MO). *N*-Phenyl-1-naphthylamine (NPN) was purchased from Kanto Chemical (Tokyo, Japan). 1-Palmitoyl-2-{6-[(7-nitrobenz-2-oxa-1,3-diazol-4-yl)amino]caproyl}-L-α-phosphatidylcholine (C_6-NBD-PC) was obtained from Invitrogen (Carlsbad, CA). Calcein and spectrograde organic solvents were supplied by Dojindo (Kumamoto, Japan). Phosphate-buffered saline (pH 7.4) for measurements of hemolysis was purchased from Sigma. All other chemicals were of special grade and were obtained from Wako (Tokyo, Japan).

Antimicrobial Activity. The minimal inhibitory concentrations (MICs) of the peptides were determined as follows. *Escherichia coli* (ATCC25922) and *Staphylococcus epidermidis* (ATCC12228) were cultured in 3% (w/v) TSB at 37 °C overnight. To obtain mid-logarithmic phase microorganisms, aliquots of 1 mL of the cultures were then transferred to 100 mL of fresh TSB broth and incubated for 2−3 h. The cells were washed with buffer [10 mM sodium phosphate and 100 mM NaCl (pH 7.4)] and resuspended in the same buffer. The cell concentrations were estimated by measuring the optical density at 600 nm (OD_{600}). The relationship between the cell concentration and OD_{600} was predetermined as colony-forming units per milliliter (cfu/mL) = $OD_{600} \times 3.8 \times 10^8$ for *E. coli* and cfu/mL = $OD_{600} \times 1.6 \times 10^8$ for *S. epidermidis*. The suspensions were diluted to 4×10^5 cfu/mL. The inoculum (90 μL) was added to each well of 96-well plates. The peptide samples (10 μL) were added to each well and incubated at 37 °C for 3 h. TSB [6% (w/v), 100 μL] was added and the mixture incubated at 37 °C for 20 h. Cell growth was assessed by measuring the optical density of the cultures at 595 nm on a model 680 microplate reader (Bio-Rad, Hercules, CA). MIC was defined as the lowest concentration of peptide that inhibited growth.

NPN Uptake Assay. The outer membrane permeabilizing activity of peptides was investigated by NPN uptake assay (*28*). Briefly, 1 mL of an overnight culture of *E. coli* (ATCC25922) was added to 50 mL of fresh 3% (w/v) TSB medium and grown to an OD_{600} of 0.4−0.6. The cells were washed with buffer [5 mM HEPES-NaOH, 5 mM glucose, 100 mM NaCl, and 5 μM CCCP (pH 7.4)] and resuspended in the same buffer. The cell concentration was determined as described above. For fluorescence measurements, 2 mL of a cell suspension (OD_{600} = 0.5) was prepared in a cuvette and 20 μL of a 1 mM NPN solution in acetone was added followed by 20 μL of an aqueous peptide solution. The fluorescence of NPN was monitored on a Shimadzu RF-5000 spectrofluorometer at an excitation wavelength of 350 nm and emission wavelength of 420 nm at 30 °C. The maximal value of NPN uptake was determined after addition of polymixin B sulfate (0.64 mg/mL, 10 μL).

Hemolytic Activity. Human erythrocytes (blood type A) from a healthy 24-year-old male were freshly prepared prior to the experiments. The blood was centrifuged (800*g* for 10 min) and washed three times with PBS (pH 7.4) to remove plasma and the buffy coat. Erythrocyte specimens were kept on ice throughout the experiments. Various concentrations of peptides were incubated with the erythrocyte suspension [final erythrocyte concentration, 1% (v/v)] for 1 h at 37 °C. The percent hemolysis was determined from the optical density at 540 nm of the supernatant after centrifugation (800*g* for 10 min), as described elsewhere (*29*). Hypotonically lysed erythrocytes were used as the standard for 100% hemolysis.

Lipid Vesicles. Large unilamellar vesicles (LUVs) were prepared and characterized as described elsewhere (*11*). Briefly, a lipid film, after drying under vacuum overnight, was hydrated with the desired solution and vortex-mixed to produce multilamellar vesicles (MLVs). The suspension was

[1] Abbreviations: CCCP, carbonyl cyanide *m*-chlorophenylhydrazone; cfu, colony-forming unit; C_6-NBD-PC, 1-palmitoyl-2-{6-[(7-nitrobenz-2-oxa-1,3-diazol-4-yl)amino]caproyl}-L-α-phosphatidylcholine; DTT, dithiothreitol; NPN, *N*-phenyl-1-naphthylamine; EYPC, egg yolk L-α-phosphatidylcholine; EYPG, L-α-phosphatidyl-DL-glycerol enzymatically converted from EYPC; Fmoc, fluoren-9-ylmethoxycarbonyl; FTIR-PATR, Fourier transform infrared-polarized attenuated total reflection; L/P, lipid-to-peptide molar ratio; LUVs, large unilamellar vesicles; MG2, F5W-magainin 2; MIC, minimal inhibitory concentration; MLVs, multilamellar vesicles; PC, phosphatidylcholine; PG, phosphatidylglycerol; SUV, small unilamellar vesicles; TSB, trypticase soy broth.

subjected to 10 freeze−thaw cycles and then extruded through polycarbonate filters (100 nm pore size filter, 31 times). Small unilamellar vesicles (SUVs) were produced by sonication of frozen and thawed MLVs in an ice/water mixture under a nitrogen atmosphere for 15 min (5 min, three times) using a probe-type UD-201 sonicator (Tomy Seiko, Tokyo, Japan). The lipid concentration was determined in triplicate by phosphorus analysis (*30*).

Calcein Leakage. LUVs were prepared by hydrating a lipid film with a 70 mM calcein solution (pH adjusted to 7.4 with NaOH) or HEPES-NaOH buffer [10 mM HEPES, 150 mM NaCl, and 1 mM EDTA (pH 7.4)]. Vesicles containing calcein were separated from free calcein on a Bio-gel A-1.5m column. Calcein-free LUVs were mixed with dye-loaded liposomes to adjust the lipid concentration to the desired value. The release of calcein from the LUVs was fluorometrically monitored on a Shimadzu RF-5000 spectrofluorometer at an excitation wavelength of 490 nm and an emission wavelength of 520 nm at 30 °C. The maximum fluorescence intensity corresponding to 100% leakage was determined by addition of 10% (w/v) Triton X-100 (20 μL) to 2 mL of the sample. The apparent percent leakage value was calculated according to

$$\% \text{ apparent leakage} = 100(F - F_0)/(F_t - F_0) \quad (1)$$

where F and F_t denote the fluorescence intensity before and after addition of the detergent, respectively, and F_0 represents the fluorescence of intact vesicles.

Tryptophan Fluorescence. Fluorescence spectra in the range of 250−500 nm were measured at an excitation wavelength of 280 nm on a Shimadzu RF-5300 spectrofluorometer at 30 °C. The blank spectra (buffer or LUVs) were subtracted.

Pore Lifetime. Pore lifetime, τ, was evaluated by determining the extent of calcein self-quenching in the peptide-treated LUVs (*31*). After calcein-entrapped LUVs were mixed with the peptide solution, the time course of the increase in calcein fluorescence was monitored. Immediately after the apparent percent leakage value reached 60−90%, 20 mM EYPG SUVs (100 μL) were added to completely stop leakage. Aliquots of the liposome suspension (250 μL) were sampled. Triton X-100 was added to the rest of the liposome suspension to completely lyse the vesicles. The apparent retention, E, was calculated according to

$$E = (F_t - F)/(F_t - F_0) \quad (2)$$

On the other hand, the sampled liposomes were applied to a Bio-gel A-1.5m column to separate the vesicle fraction from leaked calcein, and its quenching factor (Q) was obtained by measuring the fluorescence intensity before (F_b) and after (F_a) the addition of Triton X-100.

$$Q = F_b/F_a \quad (3)$$

The Q value was plotted against the E value. The ρ value, a dimensionless parameter to describe the pore life span (*31*), was estimated from theoretical Q versus E curves for various ρ values.

$$\rho = \tau_0/(\tau + \tau_0) \quad (4)$$

where τ_0 is the time necessary for a $1/e$ reduction of the intravesicular dye concentration.

Lipid Flip-Flop. The peptide-induced lipid flip-flop was assessed as previously reported (*11*). NBD-labeled LUVs composed of EYPC and C_6-NBD-PC (99.5/0.5) were mixed with 1 M sodium dithionite and 1 M Tris ([lipid] = 40 mM and [dithionite] = 60 mM) and incubated for 15 min at 30 °C to produce inner leaflet-labeled vesicles. The vesicles were immediately separated from dithionite by gel filtration. The asymmetrically NBD-labeled LUVs were incubated with or without the peptide for various periods at 30 °C (total volume of 1.9 mL). The fraction of NBD lipids that had flopped during incubation was measured on the basis of fluorescence quenching by sodium dithionite. After the addition of EYPG SUVs (final concentration of 1 mM) and dithiothreitol (DTT, final concentration of 50 mM) to recover the barrier, 20 μL of a 1 M sodium dithionite/1 M Tris solution was added. Fluorescence was monitored at excitation and emission wavelengths of 460 and 530 nm, respectively. The peptide-induced flip-flop could not be assessed for EYPG/EYPC LUVs, because even a combination of EYPG SUVs and DTT could not stop membrane permeabilization.

Fourier Transform Infrared-Polarized Attenuated Total Reflection (FTIR-PATR) Spectroscopy. Oriented EYPG/EYPC films (1/1) containing various amounts of peptides were prepared by uniformly spreading a chloroform/methanol solution of the peptide/lipid mixture on a germanium ATR plate (80 mm × 10 mm × 4 mm) followed by gradual evaporation of the solvent. The last traces of the solvent were removed under vacuum overnight. The films were hydrated with a D_2O-soaked piece of filter paper put over the plate for 3 h. The film thickness of ~6 μm, estimated from the applied amount of lipid, was much larger than the depth of penetration of the evanescent wave (0.2−0.8 μm) in the range of 3000−800 cm^{-1}. To minimize spectral contributions of atmospheric water vapor, the instrument was purged with dry N_2 gas. FTIR-PATR measurements were carried out on a Bio-Rad FTS-3000MX spectrometer equipped with a Hg−Cd−Te detector and a PIKE horizontal ATR attachment and a KRS-5 polarizer. The total reflection number was 10 on the film side. The spectra were measured at a resolution of 2 cm^{-1} and an angle of incidence of 45° and derived from 256 co-added interferograms with the Happ−Genzel apodization function. The subtraction of the gently sloping water vapor was carried out to improve the background prior to frequency measurement. The dichroic ratio, R, defined by $\Delta A_{\parallel}/\Delta A_{\perp}$, was calculated from the polarized spectra. The absorbance (ΔA) was obtained as the area of each component band for the deconvolved amide I′ bands. The subscripts $\parallel$ and $\perp$ refer to polarized light with its electric vector parallel and perpendicular to the plane of incidence, respectively. For ATR correction, refractive indexes of 4.003 and 1.440 were used for germanium and the sample film, respectively (*32*).

RESULTS

Antimicrobial Activity. The MICs of the peptides against *E. coli* and *S. epidermidis* are summarized in Table 1. A 1/1 physical mixture of MG2 and L18W-PGLa had MIC values significantly lower than those of the individual component peptides, indicating a strong synergy, as reported previously

Table 1: Biological Activities of Peptides

peptide	MIC[c] (μM) *E. coli*	MIC[c] (μM) *S. epidermidis*	% NPN fluorescence enhancement[d]	% hemolysis[e]
MG2	20	20	27.8 ± 2.9	1.2 ± 0.8
L18W-PGLa	20	5	6.8 ± 4.5	2.0 ± 0.4
mixture[a]	2.5	2.5	47.1 ± 4.8	13.4 ± 2.5
hybrid[b]	1.25	5	78.6 ± 0.1	77.9 ± 0.1

[a] An equimolar mixture of MG2 and PGLa. [b] The concentrations are expressed as concentrations reduced to monomers. [c] Minimal inhibitory concentration. [d] Percent enhancement of NPN fluorescence as a measure of outer membrane perturbation after a 5 min incubation of *E. coli* with 12.5 μM (MG2 and L18W-PGLa) or 25 μM (mixture and hybrid) peptides. [e] Percent hemolysis after a 3 h incubation of human erythrocytes with 15.6 μM (MG2 and L18W-PGLa) or 31.2 μM (mixture and hybrid) peptides.

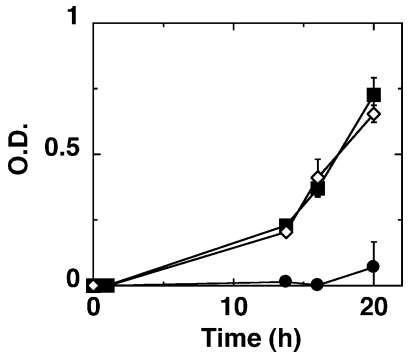

FIGURE 2: Growth inhibition against *S. epidermidis*. Cells (3.6×10^5 cfu/mL) were incubated with peptides (0.63 μM) at 37 °C. Bacterial growth was monitored by measuring the optical density at 595 nm: (◇) no peptides, (■) 1/1 mixture of MG2 and L18W-PGLa, and (●) hybrid peptide.

(*25*, *26*). The antimicrobial activity of the heterodimer was comparable to that of the mixture.

The effects of the mixture and the heterodimer on the growth rate of *S. epidermidis* were also examined at a peptide concentration (0.63 μM) well below the MICs (Figure 2). The hybrid peptide significantly inhibited the bacterial growth, whereas the mixture had no inhibitory effect.

Perturbation of the Outer Membrane. In Gram-negative bacteria, outer membranes serve as a drug barrier. Polycationic peptides were proposed to cross outer membranes by the "self-promoted uptake" mechanism (*33*). Therefore, the synergism between MG2 and L18W-PGLa in the outer membrane perturbing activity was investigated with the NPN uptake assay (*28*). NPN is normally excluded from outer membranes but is partitioned into perturbed outer membranes, exhibiting increased fluorescence. MG2 induced greater NPN uptake than L18W-PGLa, although the MICs of the two peptides were identical (Table 1). The mixture again exhibited synergy. The percent NPN uptake (47%) was larger than the arithmetic sum (34%) of the values observed for the component peptides. The NPN uptake induced by the heterodimer was significantly larger than that of the physical mixture.

Hemolytic Activity. The hemolytic activity of the peptides against human erythrocytes was determined as a measure of cytotoxicity (Table 1). MG2 and L18W-PGLa were practically nonhemolytic, whereas their equimolar mixture became weakly hemolytic under the current conditions, indicating a synergy, as observed elsewhere (*18*). In contrast, the hybrid peptide was highly hemolytic.

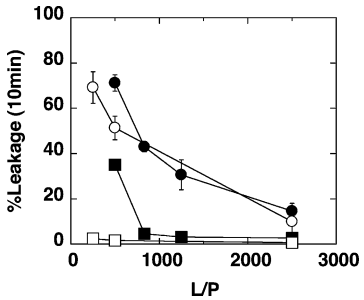

FIGURE 3: Permeabilization of phospholipid bilayers. Percent leakage values of calcein entrapped within EYPG/EYPC (filled symbols) or EYPC (empty symbols) LUVs after a 10 min incubation at 30 °C are plotted as a function of L/P ($n = 2$). The peptide concentrations are expressed as concentrations reduced to monomers: (■ and □) 1/1 mixture of MG2 and L18W-PGLa and (● and ○) hybrid peptide.

Permeabilization of Phospholipid Membranes. Phosphatidylglycerol-containing lipid bilayers are a good model for bacterial membranes and have been often used to investigate the action mechanisms of membrane-acting antimicrobial peptides (*4*, *9*, *26*, *34*−*37*). The membrane permeabilizing activities of the mixture and the heterodimer were investigated by measuring the efflux of the fluorescent dye calcein, entrapped within LUVs composed of EYPG and EYPC (1/1). The heterodimer induced calcein leakage even at a very high lipid-to-peptide molar ratio (L/P), 2500, where the equimolar mixture did not cause detectable leakage (Figure 3, filled symbols). The membrane permeabilizing activity of the hydrid peptide was also significantly larger at a lower L/P, 500. The stronger leakage activity of the heterodimer was manifested against EYPC liposomes mimicking erythrocyte membranes. The physical mixture did not induce leakage even at a L/P of 250, whereas the heterodimer started to permeabilize EYPC bilayers at a L/P of 2500 (Figure 3, empty symbols). The leakage activity of the dimer against the zwitterionic liposomes was very similar to that against the negatively charged membranes. Note that the heterodimer was completely membrane-bound under the experimental conditions used in the leakage experiments (vide infra).

Tryptophan Fluorescence. The binding affinity of the peptides for EYPG/EYPC (1/1) LUVs and the depth of the Trp residues in the membranes were estimated on the basis of Trp fluorescence. The original PGLa without Trp was used to simplify the interpretation. Peptide solutions were titrated with LUVs, and the wavelength of maximal intensity was plotted as a function of L/P (Figure 4). The binding caused a blue shift of Trp fluorescence from 352 to 334−336 nm, indicating that the Trp residues are embedded in hydrophobic environments near the membrane surface. The wavelength for the hybrid peptide was identical to that of the physical mixture of MG2 and PGLa. The wavelength for MG2 was slightly (∼2 nm) red-shifted compared to that of the dimer or the mixture, suggesting a shallower penetration of MG2. The rank order in terms of affinity for the bilayer was as follows: dimer > mixture > MG2 (as judged from the L/P dependence of the fluorescence).

The binding of the peptides to zwitterionic EYPC bilayers was also assessed on the basis of Trp fluorescence. For the dimer, addition of the liposomes caused a blue shift of Trp

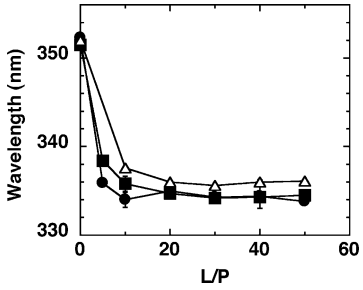

FIGURE 4: Changes in Trp fluorescence upon binding of the peptides to EYPG/EYPC (1/1) LUVs. Peptide solutions (2 μM as Trp) were titrated with LUVs at 30 °C. The wavelength of maximal intensity is plotted as a function of L/P. The peptide concentrations are expressed as concentrations reduced to monomers. The data are the averages of two independent preparations for each type of sample. Error bars indicate the standard deviation: (△) MG2, (■) 1/1 mixture of MG2 and PGLa, and (●) hybrid peptide.

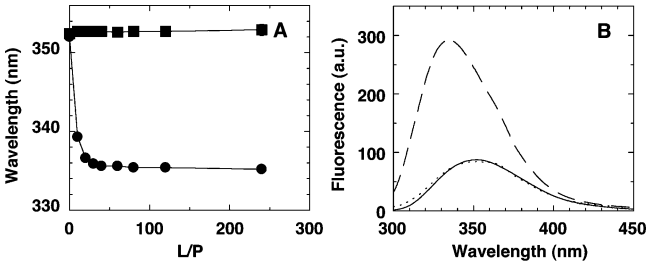

FIGURE 5: Changes in Trp fluorescence upon binding of the peptides to EYPC LUVs at 30 °C. (A) Peptide solutions (4 μM) were titrated with LUVs at 30 °C. The peptide concentrations are expressed as concentrations reduced to monomers. The wavelength of maximal intensity is plotted as a function of L/P. The data are the averages of two independent preparations for each type of sample. Error bars indicate the standard deviation: (■) 1/1 mixture of MG2 and PGLa and (●) hybrid peptide. (B) Fluorescence spectra of the hybrid peptide (4 μM) measured in buffer (—), in the presence of 400 μM EYPC membranes (− − −), and in the presence of both EYPC and 40 mM DTT (···).

fluorescence from 352 to 335 nm (Figure 5A), as in the case of the negatively charged membranes (Figure 4). The affinity for EYPC was smaller than that for EYPG/EYPC membranes, because the fluorescence did not reach a plateau until the L/P equaled 40. In contrast, the physical mixture of MG2 and PGLa did not bind to EYPC liposomes, consistent with no leakage (Figure 3B). To confirm that such a difference between the dimer and the mixture is not due to the presence of the GGC extension in the dimer, reduction experiments were performed (Figure 5B). The treatment of the dimer−lipid complex with the reducing agent DTT almost completely reverted the level of fluorescence to that in buffer, indicating that the mixture of the reduced peptides shows no affinity for EYPC bilayers, like the mixture of MG2 and PGLa.

Pore Lifetime. The lifetime of pores formed by the hybrid peptide in EYPC membranes was estimated on the basis of self-quenching of calcein according to the method of Schwarz and Arbuzova. (*31*). However, it could not be determined for EYPG/EYPC LUVs, because the binding of the peptide to the membrane was too tight to stop leakage by conventional treatment with trypsin or excess EYPG SUVs. The quenching factor (Q) of calcein is plotted against the apparent retention of calcein (E) in Figure 6. The ρ value was estimated to be 0.1 ± 0.1 by comparison of the data with the theoretical curves, corresponding to $\tau = 9\tau_0$. Thus, the pore is relatively stable compared to that formed by an

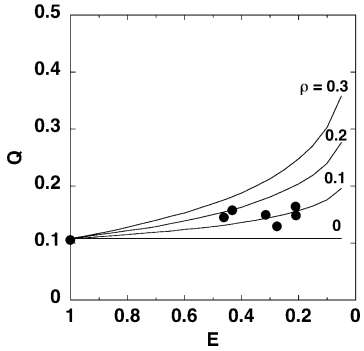

FIGURE 6: Lifetime of pores formed by the MG2−PGLa hybrid peptide in EYPC LUVs at 30 °C. The apparent calcein retention, E, is shown against the quenching factor, Q. Theoretical curves for $\rho = 0$, 0.1, 0.2, and 0.3 calculated according to Schwarz and Arbuzova (*31*) are also shown.

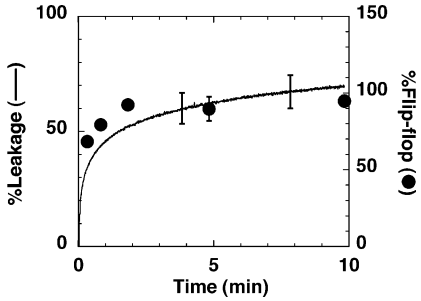

FIGURE 7: Coupling between pore formation and lipid flip-flop at 30 °C. Calcein leakage and lipid flip-flop induced by the MG2−PGLa hybrid peptide (0.2 μM) against EYPC LUVs (50 μM) are shown as a function of time ($n = 2$). The peptide concentration is expressed as a concentration reduced to monomers.

equimolar mixture of MG2 and PGLa in EYPG/EYPC LUVs ($0.7\tau_0$), assuming the same τ_0 value for the two membrane systems (*26*).

Lipid Flip-Flop. EYPC LUVs with inner leaflets labeled with C_6-NBD-PC were used to detect flip-flop of membrane lipids induced by the hybrid peptide. The percent flip-flop value when L/P = 250 is plotted as a function of time in Figure 7. The time course of the flip-flop was similar to that of calcein leakage, indicating a coupling between pore formation and lipid flip-flop, similar to that of each component peptide (*26*).

FTIR-PATR. The conformation and orientation of the peptides in EYPG/EYPC membranes (1/1) were estimated on the basis of FTIR-PATR measurements (Table 2). In all cases, the lipids in the fluid state were well-aligned (average orientational angles of acyl chains were 35−40°), as judged from the dichroic ratios of CH_2 asymmetric stretching vibration bands around 2853 cm^{-1}. The peptides exhibited amide I′ peaks in the wavenumber region of 1650−1654 cm^{-1}, indicating α-helical structures (*32*, *38*). The dichroic ratio R can be used to determine the orientation of the transition dipoles, and therefore the helix axis (*32*). Using an angle θ of 35° between the helix axis and the transition moments (*39*), the molecular orientation angle, α, around the membrane normal was calculated (*40*).

$$\cos^2 \alpha = \frac{1}{3}\left(\frac{4}{3\cos^2 \theta - 1} \times \frac{R - 2.00}{R + 1.45} + 1\right) \qquad (5)$$

MG2 and L18W-PGLa assumed surface orientations ($\alpha \sim 70°$) even at a low L/P value of 20 (Table 2). The

Table 2: Conformation and Orientation of the Peptides in Lipid Bilayers

lipid	peptide	L/P[a]	wavenumber (cm^{-1})[b]	R[c]	α (deg)[d]
EYPG/EYPC	MG2	20	1650	1.47	72
	L18W-PGLa	20	1653	1.59	67
	mixture	20	1653	1.64	65
		50	1654	1.44	74
	hybrid	50	1653	1.70	63
		100	1654	1.69	63
EYPC		50	1655	2.22	50

[a] Lipid-to-peptide molar ratio. The peptide concentrations are expressed as concentrations reduced to monomers. [b] Peak wavenumber of the amide I′ band. Errors in duplicated experiments were within 1 cm^{-1}. [c] Dicroic ratio. Errors in duplicated experiments were within 0.1. [d] Angle between the helix axis and the membrane normal evaluated with eq 5 ($\theta = 35°$).

orientation did not strongly depend on L/P. A similar α value of 74° was observed for MG2 at a higher L/P value of 40 (*41*). The hybrid peptide took a more oblique orientation irrespective of L/P values. The orientation of the mixed peptides was dependent on L/P. At a higher value, the orientation was similar to that of MG2, whereas the α value approached that of the hybrid peptide with a decrease in L/P, suggesting that the population of the MG2−PGLa complex in the peptide mixture increases with peptide concentration.

For the hybrid peptide, FTIR spectra were also measured in EYPC bilayers (Table 2). The peptide also assumed an α-helix. However, the orientational angle was significantly reduced to 50°.

DISCUSSION

Our hypothesis for the mechanism of synergism between magainin 2 and PGLa is that a 1/1 stoichiometric complex of the peptides composed of parallel helices is formed in the membrane in a concentration-dependent manner and the complex possesses potent membrane permeabilizing activity (*26*, *27*). The results of the current study fully support this model. The antimicrobial activity (Figure 2) and the leakage activity against negatively charged membranes (Figure 3) of the hybrid peptide were much stronger than those of the physical mixture of the component peptides at lower concentrations, where complex formation is suppressed. At higher concentrations where the heterodimerization is facilitated, the penetration depth (Figure 4), the orientation (Table 2), and the leakage activity against EYPG/EYPC membranes (Figure 3) of the mixture approached those of the hybrid peptide. Thus, the hybrid peptide used here appears to mimic the putative magainin 2−PGLa complex and therefore should be useful for revealing the molecular mechanism of synergism.

Our previous study showed that the complex induces lipid flip-flop coupled to the formation of pores in EYPG/EYPC membranes, as in the component peptides, indicating the formation of a toroidal pore (*26*). Fluorescence (Figure 4) and FTIR (Table 2) data show that the complex more deeply and obliquely penetrated the membrane than did the component peptides that essentially lie parallel to the membrane surface. A recent ^2H NMR study also reported that PGLa alone lies at the surface, whereas the complex is inserted in dimyristoylphosphatidylglycerol/dimyristoylphosphatidylcholine bilayers (*42*), although the tilt angle of the complex was smaller than our observation. The difference may be due to differences in physicochemical properties between the two membrane systems, such as hydrocarbon thickness and fluidity.

The hybrid peptide exhibited a much stronger interaction with zwitterionic EYPC membranes (Figures 3−5) and erythrocytes (Table 1) than the 1/1 mixture of the component peptides, because the entropy in solution is largely reduced by the cross-linking of the two molecules; therefore, a larger free energy gain is obtained upon membrane binding. In contrast, in negatively charged membranes, electrostatic attraction significantly contributes to the binding energy. Hypothetical interaction of the magainin 2−PGLa complex with zwitterionic membranes can be experimentally determined using the hybrid peptide. The heterodimer also forms a toroidal pore (Figure 7). The helix is more tilted (Table 1) and the pore more stable (Figure 6) than in EYPG/EYPC membranes (*26*), probably because electrostatic interaction between the positively charged peptide and the negatively charged membrane inhibits deep insertion of the peptide (*43*). Enhanced leakage against zwitterionic membranes has been also observed for melittin (*44*) and a His-containing peptide (*45*).

The antimicrobial peptide distinctin (5.4 kDa) from the tree frog *Phyllomedusa distincta* is similar to our hybrid peptide in that it comprises two different peptides connected by an intramolecular disulfide bridge (*44*). If *X. laevis* produced a magainin−PGLa heterodimer analogous to distinctin, the peptide would be potently antimicrobial but highly cytotoxic at the same time (Table 1). Thus, the separate production of mutually recognizing peptides appears to be a good way to increase the therapeutic index that nature selected.

REFERENCES

1. Zasloff, M. (2002) Antimicrobial peptides of multicellular organisms, *Nature 415*, 389−395.
2. Hancock, R. E. W., and Sahl, H.-G. (2006) Antimicrobial and host-defense peptides as new anti-infective therapeutic strategies, *Nat. Biotechnol. 24*, 1551−1557.
3. Dürr, U. H., Sudheendra, U. S., and Ramamoorthy, A. (2006) LL-37, the only human member of the cathelicidin family of antimicrobial peptides, *Biochim. Biophys. Acta 1758*, 1408−1425.
4. Matsuzaki, K. (1998) Magainins as paradigm for the mode of action of pore forming polypeptides, *Biochim. Biophys. Acta 1376*, 391−400.
5. Zasloff, M. (1987) Magainins, a class of antimicrobial peptides from *Xenopus* skin: Isolation, characterization of two active forms, and partial cDNA sequene of a precursor, *Proc. Natl. Acad. Sci. U.S.A. 84*, 5449−5453.
6. Hoffmann, W., Richter, K., and Kreil, G. (1983) A novel peptide designated PYLa and its precursor as predicted from cloned mRNA of *Xenopus laevis* skin, *EMBO J. 2*, 711−714.
7. Matsuzaki, K. (1999) Why and how are peptide−lipid interactions utilized for self-defence? Magainins and tachyplesins as archetypes, *Biochim. Biophys. Acta 1462*, 1−10.
8. Matsuzaki, K. (2001) Molecular mechanisms of membrane perturbation by antimicrobial peptides, in *Development of Novel Antimicrobial Agents: Emerging Strategies* (Lohner, K., Ed.) pp 167−181, Horizon Scientific Press, Wymondham, U.K.
9. Matsuzaki, K., Murase, O., Tokuda, H., Funakoshi, S., Fujii, N., and Miyajima, K. (1994) Orientational and aggregational states of magainin 2 in phospholipid bilayers, *Biochemistry 33*, 3342−3349.
10. Matsuzaki, K., Sugishita, K., Ishibe, N., Ueha, M., Nakata, S., Miyajima, K., and Epand, R. M. (1998) Relationship of membrane curvature to the formation of pores by magainin, *Biochemistry 37*, 11856−11863.

11. Matsuzaki, K., Murase, O., Fujii, N., and Miyajima, K. (1996) An antimicrobial peptide, magainin 2, induced rapid flip-flop of phospholipids coupled with pore formation and peptide translocation, *Biochemistry 35*, 11361−11368.
12. Ludtke, S. J., He, K., Heller, W. T., Harroun, T. A., Yang, L., and Huang, H. W. (1996) Membrane pores induced by magainin, *Biochemistry 35*, 13723−13728.
13. Matsuzaki, K., Murase, O., Fujii, N., and Miyajima, K. (1995) Translocation of a channel-forming antimicrobial peptide, magainin 2, across lipid bilayers by forming a pore, *Biochemistry 34*, 6521−6526.
14. Matsuzaki, K., Murase, O., and Miyajima, K. (1995) Kinetics of pore formation induced by an antimicrobial peptide, magainin 2, *Biochemistry 34*, 12553−12559.
15. Hara, T., Kodama, H., Kondo, M., Wakamatsu, K., Takeda, A., Tachi, T., and Matsuzaki, K. (2001) Effect of peptide dimerization on pore formation: Antiparallel disulfide-dimerized magainin 2 analog, *Biopolymers 58*, 437−446.
16. Porcelli, F., Buck-Koehntop, B. A., Thennarasu, S., Ramamoorthy, A., and Veglia, G. (2006) Structures of the dimeric and monomeric variants of magainin antimicrobial peptides (MSI-78 and MSI-594) in micelles and bilayers, determined by NMR spectroscopy, *Biochemistry 45*, 5793−5799.
17. Mor, A., Hani, K., and Nicolas, P. (1994) The vertebrate peptide antibiotics dermaseptins have overlapping structural features but target specific microorganisms, *J. Biol. Chem. 269*, 31635−31641.
18. Kobayashi, S., Hirakura, Y., and Matsuzaki, K. (2001) Bacteria-Selective Synergism between the Antimicrobial Peptides α-Helical Magainin 2 and Cyclic β-Sheet Tachyplesin I: Toward Cocktail Therapy, *Biochemistry 40*, 14330−14335.
19. Yan, H., and Hancock, R. E. W. (2001) Synergistic interactions between mammalian antimicrobial defense peptides, *Antimicrob. Agents Chemother. 45*, 1558−1560.
20. Yang, S. T., Shin, S. Y., Hahm, K. S., and Kim, J. I. (2006) Different modes in antibiotic action of tritrpticin analogs, cathelicidin-derived Trp-rich and Pro/Arg-rich peptides, *Biochim. Biophys. Acta 1758*, 1580−1586.
21. Rosenfeld, Y., Barra, D., Simmaco, M., Shai, Y., and Mangoni, M. L. (2006) A synergism between temporins toward Gram-negative bacteria overcomes resistance imposed by the lipopolysaccharide protective layer, *J. Biol. Chem. 281*, 28565−28574.
22. Williams, R. W., Starman, R., Taylor, K. M. P., Gable, K., Beeler, T., and Zasloff, M. (1990) Raman spectroscopy of synthetic antimicrobial frog peptides magainin 2a and PGLa, *Biochemistry 29*, 4490−4496.
23. de Waal, A., Vaz Gomes, A., Mensink, A., Grootegoed, J. A., and Westerhoff, H. V. (1991) Magainins affect respiratory control, membrane potential and motility of hamster spermatozoa, *FEBS Lett. 293*, 219−223.
24. Vaz Gomes, A., de Waal, A., Berden, J. A., and Westerhoff, H. V. (1993) Electric potential, cooperativity, and synergism of magainin peptides in protein-free liposomes, *Biochemistry 32*, 5365−5372.
25. Westerhoff, H. V., Zasloff, M., Rosner, J. L., Hendler, R. W., de Waal, A., Vaz Gomes, A., Jongsma, A. P. M., Riethorst, A., and Juretić, D. (1995) Functional synergism of the magainins PGLa and magainin-2 in *Escherichia coli*, tumor cells and liposomes, *Eur. J. Biochem. 228*, 257−264.
26. Matsuzaki, K., Mitani, Y., Akada, K., Murase, O., Yoneyama, S., Zasloff, M., and Miyajima, K. (1998) Mechanism of synergism between antimicrobial peptides magainin 2 and PGLa, *Biochemistry 37*, 15144−15153.
27. Hara, T., Mitani, Y., Tanaka, K., Uematsu, N., Takakura, A., Tachi, T., Kodama, H., Kondo, M., Mori, H., Otaka, A., Fujii, N., and Matsuzaki, K. (2001) Heterodimer formation between the antimicrobial peptides magainin 2 and PGLa in lipid bilayers: A cross-linking study, *Biochemistry 40*, 12395−12399.
28. Zhang, L., Benz, R., and Hancock, R. E. W. (1999) Influence of proline residues on the antibacterial and synergistic activities of α-helical peptides, *Biochemistry 38*, 8102−8111.
29. Matsuzaki, K., Handa, T., Miyajima, K., Mikura, Y., Shimizu, H., and Toguchi, H. (1988) Quantitative analysis of hemolytic action of lysophosphatidylcholines *in vitro*: Effect of acyl chain structure, *Chem. Pharm. Bull. 36*, 4253−4260.
30. Bartlett, G. R. (1959) Phosphorus assay in column chromatography, *J. Biol. Chem. 234*, 466−468.
31. Schwarz, G., and Arbuzova, A. (1995) Pore kinetics reflected in the dequenching of a lipid vesicle entrapped fluorescent dye, *Biochim. Biophys. Acta 1239*, 51−57.
32. Goormaghtigh, E., Raussens, V., and Ruysschaert, J.-M. (1999) Attenuated total reflection infrared spectroscopy of proteins and lipids in biological membranes, *Biochim. Biophys. Acta 1422*, 105−185.
33. Hancock, R. E. W., and Chapple, D. S. (1999) Peptide antibiotics, *Antimicrob. Agents Chemother. 43*, 1317−1323.
34. Hancock, R. E. W., and Rozek, A. (2002) Role of membranes in the activities of antimicrobial cationic peptides, *FEMS Microbiol. Lett. 206*, 143−149.
35. Yeaman, M. R., and Yount, N. Y. (2003) Mechanisms of antimicrobial peptide action and resistance, *Pharmacol. Rev. 55*, 27−55.
36. Boland, M. P., and Separovic, F. (2006) Membrane interactions of antimicrobial peptides from Australian tree frogs, *Biochim. Biophys. Acta 1758*, 1178−1183.
37. Imura, Y., Nishida, M., and Matsuzaki, K. (2007) Action mechanism of PEGylated magainin 2 analogue peptide, *Biochim. Biophys. Acta 1768* 2578−2585.
38. Tatulian, S. A. (2003) Attenuated total reflection Fourier transform infrared spectroscopy: A method of choice for studying membrane proteins and lipids, *Biochemistry 42*, 11898−11907.
39. Fraser, R. D. B., and MacRae, T. P. (1973) *Conformation in fibrous proteins and related polypeptides*, Academic Press, New York.
40. Yano, Y., Takemoto, T., Kobayashi, S., Yasui, H., Sakurai, H., Ohashi, W., Niwa, M., Futaki, S., Sugiura, Y., and Matsuzaki, K. (2002) Topological stability and self-association of a completely hydrophobic model transmembrane helix in lipid bilayers, *Biochemistry 41*, 3073−3080.
41. Kobayashi, S., Chikushi, A., Tougu, S., Imura, Y., Nishida, M., Yano, Y., and Matsuzaki, K. (2004) Membrane translocation mechanism of the antimicrobial peptide buforin 2, *Biochemistry 43*, 15610−15616.
42. Tremouilhac, P., Strandberg, E., Wadhwani, P., and Ulrich, A. S. (2006) Synergistic transmembrane alignment of the antimicrobial heterodimer PGLa/magainin, *J. Biol. Chem. 281*, 32089−32094.
43. Bechinger, B. (2005) Detergent-like properties of magainin antibiotic peptides: A ^{31}P solid-state NMR spectroscopy study, *Biochim. Biophys. Acta 1712*, 101−108.
44. Benachir, T., and Lafleur, M. (1995) Study of vesicle leakage induced by melittin, *Biochim. Biophys. Acta 1235*, 452−460.
45. Vogt, T. C., and Bechinger, B. (1999) The interactions of histidine-containing amphipathic helical peptide antibiotics with lipid bilayers. The effects of charges and pH, *J. Biol. Chem. 274*, 29115−29121.

BI701850M